



RESEARCH ARTICLE

ANALYSIS OF TiFe INTERMETALLIC COMPOUND BY DFT

Emre TAŞ^{*1}, İlknur KARS DURUKAN², Yasemin ÖZTEKİN ÇİFTÇİ³

¹Gazi University, Faculty of Sciences, Department of Physics, 06500, Ankara, emre.tas@gazi.edu.tr,
ORCID: 0000-0003-2527-9434

²Gazi University, Faculty of Sciences, Department of Physics, 06500, Ankara, ilknurdurukan@gazi.edu.tr,
ORCID: 0000-0001-5697-0530

³Gazi University, Faculty of Sciences, Department of Physics, 06500, Ankara, yasemin@gazi.edu.tr,
ORCID: 0000-0003-1796-0270

Receive Date: 04.12.2022

Accepted Date: 27.03.2023

ABSTRACT

The structural, mechanical, anisotropy, and optical properties of the TiFe compound, which is the effective hydrogen storage material, were analyzed using the DFT method with the CASTEP program. The elastic constants of the cubic system, which have been determined by the stress-strain method, are stable according to the Born stability criteria. According to the mechanical properties, the compound was brittle and hard. Anisotropy properties were examined in 2D and 3D with the EIAM code. Finally, the optical properties using the complex dielectric function based on the electronic structure of TiFe; parameters such as dielectric constants, reflectivity, extinction coefficient, refractive index, and loss function were examined in the range of 0-50 eV. Generally, our obtained results are comparable with literature values.

Keywords: *Anisotropy, Hard Material, Brittle, Optic Properties.*

1. INTRODUCTION

Today, the rapid development of technology, in parallel with the increasing population, has brought the need for energy and fuel [1]. Over the years, this energy need has turned from solid-source coal to liquid-source oil and natural gas. All these fossil fuels pollute the air by releasing CO, CO₂, NO_x, and SO_x. While air pollution threatens all life, oil spills also threaten aquatic life. In addition to all these negativities, it is necessary to meet the increasing energy and fuel needs. Unfortunately, the oil will not meet the world's energy needs in the coming years.

Hydrogen is an environmentally friendly fuel with a high potential to meet the world's energy needs [2,3]. However, hydrogen is an energy carrier, not an energy source like oil; not available directly [4,5]. Although it can be produced using other sources, it must be transported and stored after being built. Today, hydrogen storage materials have become attractive to many researchers due to their

applications in the energy field. Hydrogen storage materials are material classes whose primary material is metal [6,7].

Generally, B2-type intermetallic compounds can be used for technological applications such as energy and optoelectronics due to having a high melting point and ordering energy and showing high strength, good corrosion resistance, and high phase stability [8]. Ti compounds with a B2 structure are the most widely used hydrogen storage material [9]. In addition, the partially filled d states of Ti-based compounds add extraordinary properties to the compounds formed. Titanium is particularly interested in the aerospace industry and high-friction materials [10]. In particular, TiFe is one of the most attractive materials due to its abundant and low-cost raw material, high strength, and mild hydrogenation conditions [11]. For this reason, we have attempted to review many theoretical and experimental studies on TiFe intermetallic compounds in the literature. Pawar et al. investigated the structural, electronic, phonon, and superconductivity properties of TiFe compounds using the QUANTUM ESPRESSO code based on the DFT method. They found that the compound is metallic and thermodynamically stable, and the transition temperature to superconductivity is 1.15 K [10]. Ko et al. calculated the role of ternary alloying elements in TiFe-based hydrogen storage alloys with the DFT-based VASP code. This study analyzed the effect of ternary elements on hydrogen storage with pressure composition and temperature curves [12]. Ciric et al. synthesized $\text{TiFe}_{1-x}\text{Ni}_x$ (X:0.2-0.6) by melt spinning. They analyzed the crystal structure, bond structure, and hybridization properties by varying the Fe and Ni concentration ratios. In this study, they determined that the increase in Ni concentration leads to a shift in hydrogen desorption temperatures to higher values and a decrease in the maximum amount of hydrogen absorbed under the same conditions [13]. Fodorougbo et al. analyzed the hydrogen production properties of $\text{TiFe}_{1-x}\text{M}_x$ (M=Al, Be, Co, Cr, Cu, Mn, and Ni) compounds in the light of activation, kinetic and thermodynamic properties by DFT [14]. Sujan et al. evaluated the fabrication process of TiFe intermetallic compounds from fabrication to hydrogen storage in detail.[15] Kong et al. calculated the electronic and thermodynamic properties of TiM (M: Fe, Ru, and Os) compounds using the CASTEP code based on the DFT method. They determined the sensitivity of the thermal expansion coefficient at high temperature-high pressure, where the compounds are thermodynamically stable, and that this coefficient decreases with increasing pressure.[16] Bakulin et al. investigated the effect of impurities on the diffusivity of TiFe compounds by DFT. They found that impurities change the hydrogen absorption energy at the nearest positions and neighborhoods [17]. Eladati et al. studied the effect of plastic deformation on hydrogen storage and microstructure of $\text{TiFe}_{1-x}\text{Mn}_x$ (x: 0, 0.15, and 0.3) compounds. Since the hydrogen storage performance is due to lattice defects and amorphous regions, it was determined that adding Mn expands the lattice and reduces the hydride formation energy, thereby lowering the hydrogenation/activation pressure [18]. Oliveira et al. experimentally determined hydrogen desorption kinetics at room temperature and hydrogen absorption kinetics for a cold-rolled TiFe IMC alloy processed under an inert atmosphere.[19] Dematteis et al. experimentally prepared TiFe-based alloys and provided information on the kinetics of adding Mn and copper in hydrogen storage. They also emphasized that the prepared samples have fast kinetics and high hydrogen storage properties [20]. Du et al. experimentally and theoretically analyzed the thermophysical properties of TiFe alloys [21]. In another experimental study, Yang et al. determined the microstructure and hydrogen storage properties of chromium, manganese, and irium elements in TiFe-based alloys [22].

Conventional experimental methods allow us to grasp and evaluate general changes caused by element substitution. Still, changes at a much more fundamental level are beyond the reach of standard experimental tools. In this sense, computational approaches, such as first-principle density functional theory (DFT) calculations, are of great interest as they allow better evaluation and monitoring of even small changes in good physical properties. Due to its widespread use in technology, the TiFe compound has attracted the attention of many experimental and theoretical working groups. Many studies have continued in this direction, especially after the use of TiFe intermetallic compound in hydrogen energy became known. Hydrogen-storing compounds with a B2-type structure utilizes the interatomic hydrogen storage mechanism. When hydrogen atoms are inserted into compounds, the lattice structure of the compound is disrupted by high temperature and pressure. Due to these changes during the hydrogen absorption and desorption, the material can be affected by elastic and plastic deformation. In the cycling process of hydrogen storage for the materials, poor plasticity can cause residual stress accumulates and defects which affect hydrogen storage performance. So mechanical properties of hydrogen storage material significantly affect the hydrogen storage performance. Selecting suitable materials to meet renewable energy needs is science's center. To expand this problem in a certain way, obtaining and optimizing the available materials is necessary. Optical properties need to be discussed because these properties are helpful to understand better the fundamental properties such as crystal vibrations, excitons, impurity levels, localized defects, and band structure to understand optical switching and optoelectronics applications. The optical properties of the material are attributed to electronic properties. Besides all these known facts, some physical properties of TiFe intermetallic compounds have not been observed. To contribute to the literature, TiFe compound was examined theoretically. Structural, Elastic, anisotropic and optical properties were analyzed in detail with the CASTEP program using the DFT based on the first-principles method. Before the synthesis procedure, utilizing such calculations, a very time-consuming effort, is very important.

2. MATERIAL METHOD

The structural, elastic, anisotropy, and optical properties of TiFe compound have been calculated using the Ab initio method. Ab-initio is essential in determining many macroscopic properties important in technology based on fundamental quantum mechanical theory. The main advantage of ab-initio approaches is their independence from experimental data. When appropriate algorithms and software using ab-initio calculation methods are used, results close to experimental values can be obtained. The CASTEP package program used density functional theory (DFT) [23,24] to perform all calculations. Plane-wave basis sets with 300 eV energy cutoff and 10x10x10 Monkhorst and Pack [25] k-points in the Brillouin region are used for the TiFe compound. Interactions between ions and electrons were captured using Ultrasoft Vanderbilt pseudopotential [26,27]. The electronic valence configurations for each atomic species were chosen as Ti: $3d^2 4s^2$, Fe: $3d^6 4s^2$. The parameters we used in our calculations were obtained by optimizing the TiFe compound. The stress-strain method is used to estimate the elastic properties [28]. Three-dimensional representation of anisotropy properties, EIAM code [29]. Finally, optical parameters were evaluated in the 0-50 eV range.

3. RESULTS and DISCUSSION

3.1. Structural and Elastic Properties

TiFe is found in 221 space groups in the CsCl structure. The representation of the atoms in the compound in the unit cell is as Fe atom in the center and Ti atom at the corners. It is presented in Fig. 1a. The Bulk modulus and first derivative were calculated by fitting the Murnaghan equation of the graph given in Figure 1b. Structural parameters are listed in Table 1 and compared with the literature. The calculated values are comparable with previous studies [16,31-33]. It is possible to determine the material's structural stability by the formation's enthalpy.

$$\Delta H^{\text{TiFe}} = E_{\text{tot}}^{\text{TiFe}} - E_t^{\text{Ti}} - E_t^{\text{Fe}} \quad (1)$$

Here, $E_{\text{tot}}^{\text{TiFe}}$ is the total energy of TiFe per unit cell, and E_t^{Ti} , E_t^{Fe} shows the computed energies per unit cell at 0K and 0GPa. The negative ΔH is indicative of its stability and experimental feasibility. The computed formation enthalpy value of TiFe is -1.495 eV/f.u. The negative value of ΔH^{TiFe} shows the stability of TiFe thermodynamically.

Table 1. The structural parameters of TiFe.

	Lattice constant (Å)	B(GPa)	B'
TiFe	2.960	182.34	3.90
Ref.	2.961[16]	174.64[16]	2.135[16]
	2.978[1]		
	2.969[2]		
	2.965[3]		

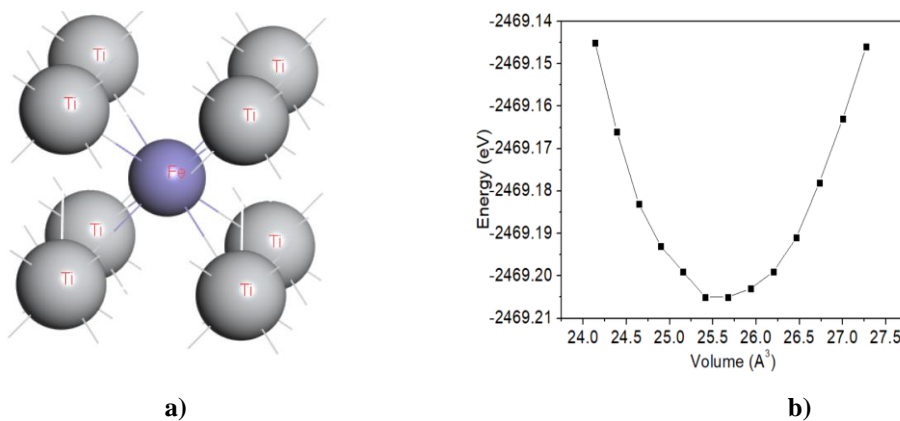


Figure 1. a) The unitcell of TiFe, b) Total energy - volume curve.

Elastic properties, determining the physical response of the material, are fundamental in understanding its effectiveness in device applications. In addition, the thermodynamic behavior of the material can be learned by knowing the elastic properties. Three elastic constants are required for the cubic system, while the elastic properties determine the material's response to stress. C_{11} determines the presence of rigidity of the material, while C_{12} determines the transverse expansion. C_{44} is related to shear deformation. These three elastic constants are essential in determining the stability of the material. The stability conditions of the cubic system, known as the Born-Huang criteria [34], are related to fulfilling the four criteria listed below.

$$C_{11}-C_{12} > 0 \quad (2)$$

$$C_{11} > 0 \quad (3)$$

$$C_{44} > 0 \quad (4)$$

$$C_{11}+2C_{12} > 0 \quad (5)$$

The mechanical properties can be calculated by the equations presented below by determining the elastic constants [35].

$$B = \frac{1}{3}(C_{11} + 2C_{12}) \quad (6)$$

$$G = \frac{1}{5}(C_{11} - C_{12} + 3C_{44}) \quad (7)$$

$$E = \frac{9BG}{3B+G} \quad (8)$$

$$H_v = 2 \left(\left(\frac{G}{B} \right)^2 G \right)^{0.585} - 3 \quad (9)$$

$$C'' = C_{12}-C_{44}$$

$$\nu = \frac{3B-2G}{2(3B+G)} \quad (10)$$

$$A = \frac{2C_{44}}{C_{11}-C_{12}} \quad (11)$$

Elastic constants and mechanical properties are calculated and presented in Table 2. C_{11} , C_{12} , and C_{44} , satisfied the stability state. $\text{XTi}(X=\text{Fe}, \text{Co}, \text{Ni}, \text{Ru})$ compounds in the B2 structure presented in Table 2 also have stable structures [36,37]. The Bulk modulus (B, GPa) indicates the material's compressibility and ability to resist fracture. The larger this value, the more difficult it is to compress the material. The Shear module (G, GPa) defines the resistance to plastic deformation. Young's modulus (E, GPa) is the stress per unit strain mainly related to the chemical bond of the atoms in the materials. E also gives information about the hardness of the material. Because of E value, TiFe compound is hard. When compared with the $\text{XTi}(X=\text{Fe}, \text{Co}, \text{Ni}, \text{Ru})$ compounds in the literature, it

was determined by our calculations that the hardest compound was TiFe [36,37], indicating the stronger chemical bond. The ductile or brittle behavior is determined from the B/G ratio, the Paugh ratio, and C'' Cauchy pressure. If this ratio is greater than 1.75, it is ductile. Otherwise, it is brittle. It is ductile if positive for Cauchy pressure and brittle if negative. TiFe is brittle according to Cauchy pressure and Paugh ratio. However, XTi (X=Fe, Co, Ni, Ru) compounds show ductile properties in Table 2 [36,37]. The Poisson ratio (ν) describes the bonding forces in solids and is the center of interatomic force in a material if ν ranges from 0.25 to 0.50. When the ν is 0.5, the material is nearly incompressible. The forces of the TiFe and XTi(X=Fe, Co, Ni, Ru) compounds are central [36,37]. Hv is a parameter that defines the stiffness against deformation. For the B2 structure the hardness increase with constant elastic C_{44} [34]. If the value of this parameter is above 10, it is hard; if it is above 40, it is super-hard. TiFe compound has a hard structure with a value of 13.00. Higher values of the bulk modulus, shear modulus, B/G ratio, and Poisson's ratio indicate that the hydrogen enhances the ability of TiFe to resist fracture and plastic deformation and improve ductility and cycle performance. Zener anisotropy A is calculated from elastic constants. It is isotropic when this value equals 1, and anisotropic when it is small or large. TiFe and XTi(X=Fe, Co, Ni, Ru) compounds have an anisotropic nature [36,37].

Table 2. Elastic constants (C_{11} , C_{12} , C_{44}), Bulk modulus (B, GPa), Shear modulus (G, GPa), Young modulus (E, GPa), Paugh ratio (B/G), Cauchy pressure ($C''= C_{12}-C_{44}$), Poisson ratio (ν), Hardness (Hv),. Anizotropy(A) of TiFe and other compounds.

	C_{11}	C_{12}	C_{44}	B	G	E	B/G	C''	ν	Hv	A
TiFe	369.742	72.059	82.038	171.287	99.989	251.106	1.713	9.979	0.267	13	0.438
FeTi(2)	372.95	87.1	68.63	182.38	92.49	237.36	1.97	18.47	0.28		0.48
CoTi(2)	286.51	113.79	74.66	173.56	79.13	205.74	2.16	39.13	0.29		0.86
NiTi(2)	195.93	157.59	62.9	160.03	39.14	109.09	4.35	94.68	0.39		3.28
RuTi(3)	386.97	135.37	109.27	220.97	133.69	138.32	1.81	10.04	0.26		0.58

The mechanical parameters, Young's modulus (E_{\min} and E_{\max} , GPa), Shear modulus (G_{\min} and G_{\max} , GPa), and Poisson's ratio (ν_{\min} , ν_{\max}), are presented in Table 3. The minimum and maximum values of mechanical parameters are given in Table 3; all parameters are anisotropic. Mechanical parameters were plotted using the ELATE code. The mechanical parameters Young's modulus, shear modulus, and Poisson's ratio depending on the two-three-dimensional orientation, are presented in Figure 2. Deviation from sphericity in the figures indicates anisotropy; it is anisotropic like other intermetallic compounds [36,37]. Minimum values are shown in green, while maximum values are shown in blue.

Table 3. Variation of mechanical parameters.

	E_{\min} (GPa)	E_{\max} (GPa)	G_{\min} (GPa)	G_{\max} (GPa)	ν_{\min}	ν_{\max}
TiFe	212.23	346.24	82.038	148.84	0.110	0.432
Anisotropy		1.631		1.814		3.903

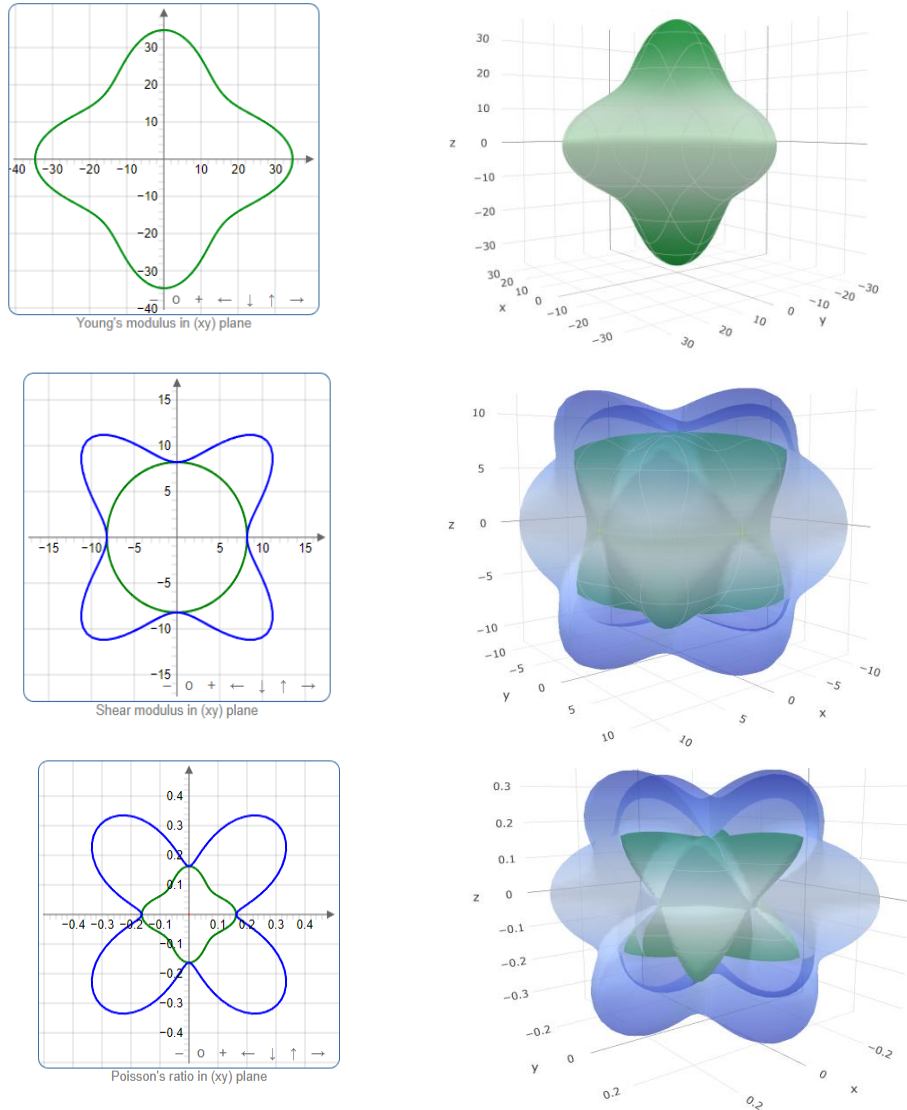


Figure 2. The Calculated two- and three-dimensional elastic anisotropy parameters of TiFe.

3.2 Optic Properties

Optical properties are the compound's response to electromagnetic waves. Optical constants are obtained using the complex dielectric function.

$$\varepsilon(E) = \varepsilon_1(E) + i \varepsilon_2(E) \quad (12)$$

It is the wave vector's polarization response to the external electromagnetic field in a given system. The photon's electric field allows transitions between the occupied and unoccupied wave vector states. $\epsilon_1(\omega)$ shows the dispersion of incoming photons by the materials, while $\epsilon_2(\omega)$ is related to the energy absorbed by the material [38]. In Fig. 3a, the variation of the real part $\epsilon_1(\omega)$ and the real part $\epsilon_2(\omega)$ of the dielectric function in the energy range from 0 to 50 eV is given. The limit value $\epsilon_1(0) = 45.73$, corresponding to the near-zero radiation frequency, is called the static dielectric constant. $\epsilon_1(\omega)$ shows that the zero crossing of the spectrum means no scattering. Between [2.86–16.71eV] and [35.86–35.35 eV], $\epsilon_1(\omega)$ exhibits negative values, in which case the compound shows metallic character [39]. The fluctuations in the dielectric function's real part indicate localized absorption and reflection maxima. The dielectric function's imaginary part $\epsilon_2(\omega)$, indicating the electronic excitations between 0 and 50 eV, was also examined. It was determined that it peaked in the visible region and took the maximum value. Values indicate optical absorption when the dielectric function is greater than zero. Absorption and reflection decrease toward zero in the UV region.

The graph of the refractive index $n(\omega)$ and the extinction coefficient $k(\omega)$ according to the energy change is given in Fig 3b. When a light beam changes medium, it changes direction, and refraction occurs due to the change in propagation speed. The behavior of the $n(\omega)$ against energy is similar to the real part of the dielectric constant. The square of the $n(\omega)$ at zero frequency equals the $\epsilon_1(\omega)$. While the points where the refractive index is maximum are in the IR region, it decreases in the Visible region and fluctuates in the UV region. The extinction coefficient peaks $k(\omega)$, which indicates the transition between bands in the range of 0-10 eV, then after 10 eV, fluctuations occur in the UV region.

In Figure 3c, the variation of the absorption of the material against the energy values indicating the portion of energy lost by the wave when passed through the material is given. The region with the highest absorption is the UV region with fluctuations in this region. The maximum absorption is 5.68 10⁵ cm⁻¹, corresponding to an energy value of 36.18 eV. These results show TiFe as a prospective material for optoelectronics in the ultraviolet region mainly due to its extremely sharp cut-off response, particularly in this region.

The reflectivity of the material, expressed as a percentage, is given in Fig 3d. $R(\omega)$ can be defined as the ratio between reflected and incident luminous flux. Different peaks are indicative of the reflection of photons from the material surface. $R(0)$ is high at zero energy, and its value is 54%. At low energies, $R(\omega)$ fluctuates and reaches a maximum of 70% in the UV range, with a maximum value of around 60% in the visible range (1.73–3.4 eV). The highest reflective region of TiFe is UV, with a reflectance value of 70 percent.

The energy loss function $L(\omega)$ is the energy loss of an electron moving through a material, indicating the energy lost by the high-speed electron, and is presented in Figure 3e. The energy loss function $L(\omega)$ has no significant peak in the visible and near-infrared regions. This situation can be interpreted as $\epsilon_2(\omega)$ showing large values in these ranges. The prominent peak in the figure is called the plasma frequency, which indicates the combined performance of the loosely bounded electrons in the valence and conduction bands. Its value is about 4.48.

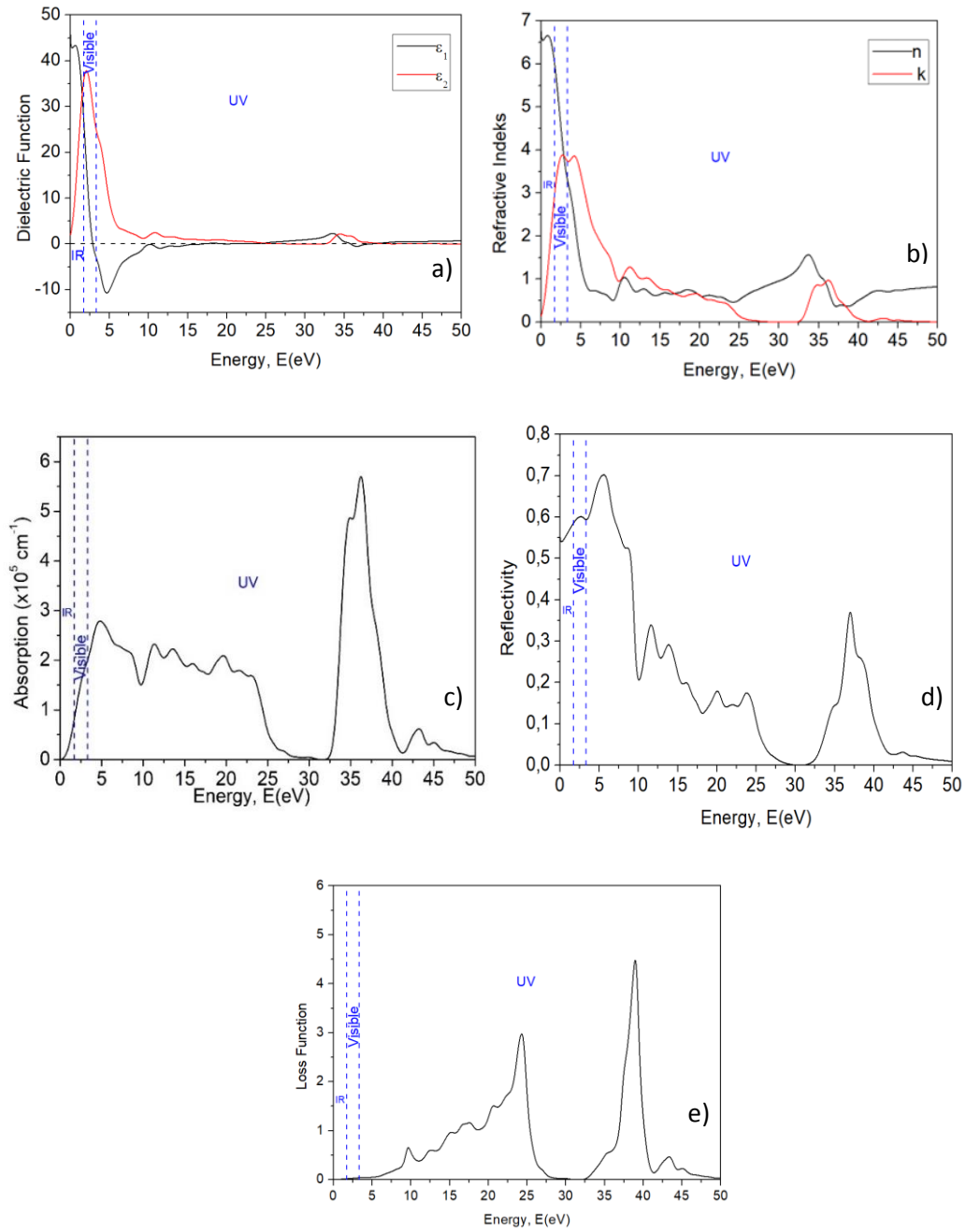


Figure 3. Optical properties of TiFe.

4. CONCLUSION

Structural, Elastic, anisotropic, and optical properties of TiFe were analyzed by the first-principles method using DFT. The CASTEP program was used in our calculations as a purely theoretical study. The structural and mechanical properties for TiFe were compared with experimental and theoretical results available in the literature. The results were found to be generally in agreement with the literature data. Second-order elastic constants and mechanical parameters of the TiFe compound at zero pressure were calculated. TiFe compound shows a hard and brittle structure. The mechanical parameters of the TiFe compound calculated with the 2D and 3D ELATE program also show anisotropy (A) properties. Optical properties were examined in the range of 0-50 eV to understand the improved application status of TiFe compound. It has a refractive index of 6.76 and a reflectivity of 70 percent in the UV region. Obtained results in this study could help improve the hydrogen storage performance of TiFe as a promising candidate for optoelectronic devices.

ACKNOWLEDGEMENT

The authors declare that they have no conflict of interest.

REFERENCES

- [1] Niaz, S., Manzoor, T., Pandith, A.H. (2015). Hydrogen storage: Materials, methods and perspectives. *Renewable and Sustainable Energy Reviews*, 50, 457-469.
- [2] Nazir, G., Tariq, S., Mahmood, Q., Saad, S., Mahmood, A., Tariq, S. (2018). Under Pressure DFT Investigations on Optical and Electronic Properties of Under Pressure DFT Investigations on Optical and Electronic Properties of PbZrO₃. *Acta Physica Polonica A*, 133, 105-113.
- [3] Veziroglu, T.N., Barbir, F. (1992). Hydrogen: the wonder fuel. *International Journal of Hydrogen Energy*, 17(6), 391-404.
- [4] Andreas, Z. (2004). Hydrogen storage methods. Published online, 91, 157-172.
- [5] Graetz, J. (2009). New approaches to hydrogen storage. *Chemical Society Reviews*, 38(1), 73-82.
- [6] Collins, D.J., Zhou, H.C. (2007). Hydrogen storage in metal – organic frameworks. *Journal of Materials Chemistry*, 17(30), 3154-3160.
- [7] Long, J.R., Murray, L.J., Dinca, M. (2009). Hydrogen storage in metal – organic frameworks. *Chemical Society Reviews*, 38(5), 1294-1314.

- [8] Kaneno, Y., Takasugi, T. (2003). Effects of microstructure and environment on room-temperature tensile properties of B2-type polycrystalline CoTi intermetallic compound. *Journal of materials science*, 38, 869-876.
- [9] Guo, Q., Kleppa, O.J. (1998). Standard enthalpies of formation of some alloys formed between group IV elements and group VIII elements, determined by high-temperature direct synthesis calorimetry II. Alloys of (Ti, Zr, Hf) with (Co, Ni). *Journal of Alloys and Compounds*, 269, 181-186.
- [10] Pawar, H., Shugani, M., Aynyas, M., Sanyal, S.P. (2019). Electronic structural, lattice dynamics and superconducting properties of tife intermetallic compound: A first-principles study. *AIP Conference Proceedings*, 2115, 030336.
- [11] Edalati, K., Matsuda, J., Arita, M., Daio, T., Akiba, E., Horita, Z. (2013). Mechanism of activation of TiFe intermetallics for hydrogen storage by severe plastic deformation using high-pressure torsion. *Applied Physics Letters*, 103, 143902.
- [12] Ko, W.S., Park, K.B., Park, H.K. (2021). Density functional theory study on the role of ternary alloying elements in TiFe-based hydrogen storage alloys. *Journal of Materials Science & Technology*, 92, 148-158.
- [13] Ćirić, K.D., Kocjan, A., Gradišek, A., Koteski, V.J., Kalijadis, A.M., Ivanovski, V.N., Laušević, Z.V., Stojić, D.L. (2012). A study on crystal structure, bonding and hydriding properties of Ti-Fe-Ni intermetallics – Behind substitution of iron by nickel. *International journal of hydrogen energy*, 37, 8408-8417.
- [14] Fadonougbo, J.O., Park, K.B., Na, T.W., Park, C.S., Park, H.K., Ko, W.S. (2022). An integrated computational and experimental method for predicting hydrogen plateau pressures of TiFe_{1-x}M_x-based room temperature hydrides. *International journal of hydrogen energy*, 47, 17673-17682.
- [15] Sujan, G.K., Pan, Z., Li, H., Liang, D., Alam, N. (2019). An overview on TiFe intermetallic for solid-state hydrogen storage: microstructure, hydrogenation and fabrication processes. *Critical Reviews in Solid State and Materials Sciences*, 45(5), 410-427.
- [16] Kong, Z., Duan, Y., Peng, M., Qu, D., Bao, L. (2019). Theoretical predictions of thermodynamic and electronic properties of TiM (M= Fe, Ru and Os). *Physica B: Condensed Matter*, 573, 13-21.
- [17] Bakulin, A.V., Kulkov, A.S., Kulkova, S.E. (2023). Impurity influence on the hydrogen diffusivity in B2-TiFe. *International journal of hydrogen energy*, 48, 232-242.
- [18] Edalati, K., Matsuo, M., Emami, H., Itano, S., Alhamidi, A., Staykov, A., Smith, D.J., Orimo, S-i., Akiba, E., Horita, Z. (2016). Impact of severe plastic deformation on microstructure and hydrogen storage of titanium-iron-manganese intermetallics. *Scripta Materialia*, 124, 108-111.

- [19] Oliveira, V.B., Beatrice, C.A.G., Leal Neto, R.M., Silva, W.B., Pessan, L.A., Botta, W.J., Leiva, D.R. (2021). Hydrogen absorption/desorption behavior of a cold-rolled tife intermetallic compound. *Materials Research*, 24(6), 2021-0204.
- [20] Dematteis, E.M., Cuevas, F., Latroche, M. (2020). Hydrogen storage properties of Mn and Cu for Fe substitution in TiFe_{0.9} intermetallic compound. *Journal of Alloys and Compounds*, 851, 156075.
- [21] Du, L.Y., Wang, L., Zhai W., Hu, L., Liu, J.M., Wei, B. (2018). Liquid state property, structural evolution and mechanical behavior of TiFe alloy solidified under electrostatic levitation condition. *Materials and Design*, 160, 48-57.
- [22] Yang, T., Wang, P., Xia, C., Liu, N., Liang, C., Yin, F., Li, Q. (2020). Effect of chromium, manganese and yttrium on microstructure and hydrogen storage properties of TiFe-based alloy. *International Journal of Hydrogen Energy*, 45, 12071-12081.
- [23] Mehmood, N., Ahmad, R., Murtaza, G. (2017). Ab Initio Investigations of Structural, Elastic, Mechanical, Electronic, Magnetic, and Optical Properties of Half-Heusler Compounds RhCrZ (Z = Si, Ge). *Journal of Superconductivity and Novel Magnetism*, 30(9), 2481-2488.
- [24] Kresse, G., Hafner, J. (1993). Ab initio molecular dynamics for liquid metals. *Physical Review B*, 47(1), 558-561.
- [25] Le Page, Y., Saxe, P. (2002). Symmetry-general least-squares extraction of elastic data for strained materials from ab initio calculations of stress. *Physical Review B - Condensed Matter and Materials Physics*, 65(10), 1-14.
- [26] Perdew, J.P., Chevary, J.A., Vosko, S.H., Jackson, K.A., Pederson, M.R., Singh, D.J., Fiolhais, C. (1992). Atoms, molecules, solids, and surfaces: Applications of the generalized gradient approximation for exchange and correlation. *Physical review B*, 46(11), 6671-6687.
- [27] Vanderbilt, D. (1990). Soft self-consistent pseudopotentials in a generalized eigenvalue formalism. *Physical review B*, 41(11), 7892-7895.
- [28] Mehl, M.J., Osburn, J.E., Papaconstantopoulos, D.A., Klein, B.M. (1990). Structural properties of ordered high-melting-temperature intermetallic alloys from first-principles total-energy calculations. *Physical Review B*, 41(15), 10311-10323.
- [29] Marmier, A., Lethbridge, Z.A.D., Walton, R.I., Smith, C.W., Parker, S.C., Evans, K.E. (2010). EIAM : A computer program for the analysis and representation of anisotropic elastic properties. *Computer Physics Communications*, 181(12), 2102-2115.
- [30] Murnaghan, F.D. (1944). The compressibility of media under extreme pressure. *Proceedings of the National Academy of Sciences*. 30(9), 244-247.

- [31] Melnyk, G., Tremel, W. (2003). The titanium–iron–antimony ternary system and the crystal and electronic structure of the interstitial compound Ti_5FeSb_2 . *Journal of alloys and compounds*, 349(1-2), 164-171.
- [32] Duwez, P., Taylor, J. (1950). The structure of intermediate phases in alloys of titanium with iron, cobalt, and nickel. *Journal of Metals*, 188, 1173-1176.
- [33] Fischer, P., Hälg, W., Schlapbach, L., Stucki, F., Andresen, A.F. (1978). Deuterium storage in FeTi. Measurement of desorption isotherms and structural studies by means of neutron diffraction. *Materials Research Bulletin*, 13(9), 931-946.
- [34] Mouhat, F., Coudert, F.X. (2014). Necessary and sufficient elastic stability conditions in various crystal systems. *Physical Review B - Condensed Matter and Materials Physics*, 90(22), 1-4.
- [35] Kars Durukan, I., Oztekin Ciftci, Y. (2020). First-principles calculations of vibrational and optical properties of half-Heusler NaScSi. *Indian Journal of Physics*, Published online, 95, 2303-2312.
- [36] Acharya, N., Fatima, B., Chouhan, S.S., Sanyal, S.P. (2013). First Principles Study on Structural , Electronic , Elastic and Thermal Properties of Equiatomic MTi (M = Fe , Co , Ni). *Chemistry and Materials Research*, 3, 22-30.
- [37] Jain, E., Pagare, G., Chouhan, S.S., Sanyal, S.P. (2014). Electronic structure, phase stability and elastic properties of ruthenium based four intermetallic compounds: Ab-initio study. *Intermetallics*, 54, 79-85.
- [38] Liu, Z.T.Y., Gall, D., Khare, S.V. (2014). Electronic and bonding analysis of hardness in pyrite-type transition-metal pernitrides. *Physical review B*, 90(13), 134102.
- [39] Anissa, B., Radouan, D., Durukan I.K. (2022). Study of structural, electronic, elastic, optical and thermoelectric properties of half - Heusler compound RbScSn: A TB - mBJ DFT study. *Optical and Quantum Electronics*, 54(6), 1-17.